Applications of Abaqus at The Timken Company

Matt Wilmer and Krich Sawamiphakdi

Timken Technology Center in North Canton, Ohio

Abstract: *At The Timken Company, Abaqus is used in both product and process development. Several examples are presented in this paper. New product applications rely on the linear and nonlinear implicit solvers of Abaqus. Examples include stiffness matrix extraction for use in Timken's SYBER™ bearing analysis program. Stiffnesses of the structural components surrounding the bearing can greatly affect bearing life. Stiffness matrices of the housing are imported into our bearing analysis code to better define roller loads and misalignment for more accurate bearing life predictions. Another example is structural analysis of bearing integrated products such as the wheel bearing/ hub assembly. New process applications rely on the Abaqus explicit solver. Examples include cold ring rolling, tube elongating and straightening processes. The explicit solver is used to decrease solve time while giving accurate analysis results. Another example is the use of Abaqus/Standard to investigate the effects of inclusions at various positions and orientations on bearing stresses. The user routine is used to specify stress boundary conditions on the model under Hertzian contact. Finite Element Analysis is an important tool that enables evaluation of product and process design before making prototypes.*

Keywords: *Finite Element Analysis, Bearing System Analysis, Metal Forming Process, Tube Making Process*

Product Modeling - Bearing/System Analysis

Structural support of bearing components is important for optimal bearing performance. Housing flexibility can have detrimental effects on bearing alignment causing high edge stresses and decreased bearing life. A system level analysis approach is the best method for determining these stresses and bearing lives. Timken's bearing analysis tool, SYBER™, has the ability to import stiffness matrices generated by Finite Element Analysis and incorporate them in the bearing life calculations. Accounting for this bearing support flexibility enables more accurate bearing alignment and stress calculations. Based on these findings, modifications can be done to the structural housing and the bearing components to optimize bearing life and total system performance (Timken, 2007) (Abaqus, 2007).

An automotive transaxle is a good example of how housing flexibility can affect bearing performance (Timken, 1985). Figure 1 shows a simple automotive transaxle that uses multiple bearings to support the geared shafts. The load and flexibility of each housing position affects each bearing misalignment. By creating an FE mesh of the housing with MPC connected to the bearing centers, a stiffness matrix can be extracted that relates the flexibility of each housing support location with each bearing. Taking into account the housing stiffness improves the bearing calculation giving a more accurate life prediction.

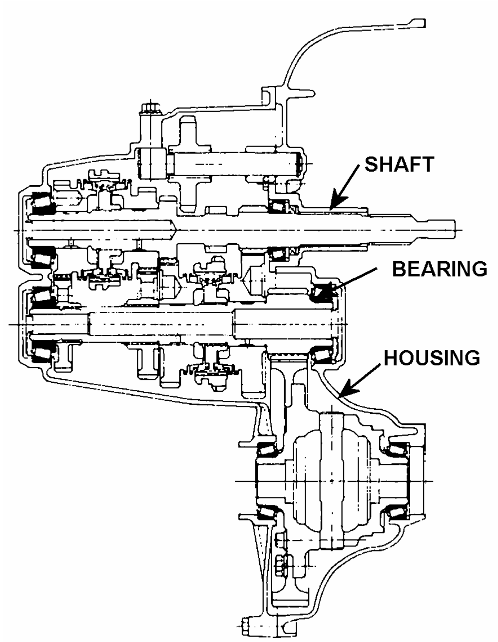

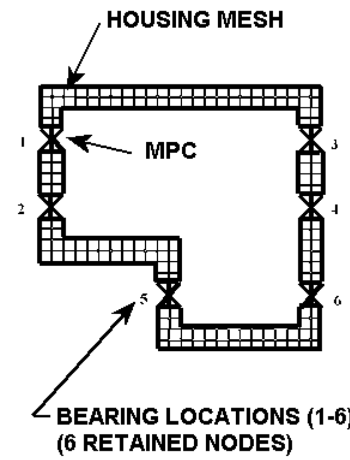

Figure 1 – Housing Stiffness Matrix Extraction for Bearing Calculation

The stiffness matrix is solved for the retained nodes at the bearing centers. This stiffness matrix is imported into the SYBER™ bearing analysis program. Bearing loads and misalignment are calculated based on the applied load and the flexibility of the housing and shaft constraints. The effect of housing stiffness can be seen in the bearing stress plots in Figure 2.

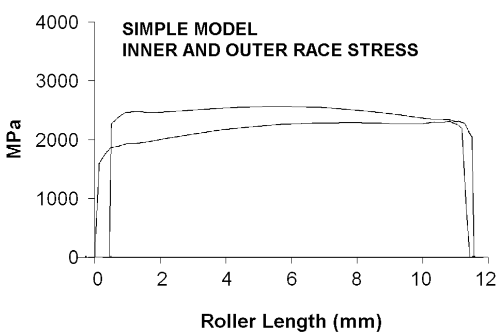

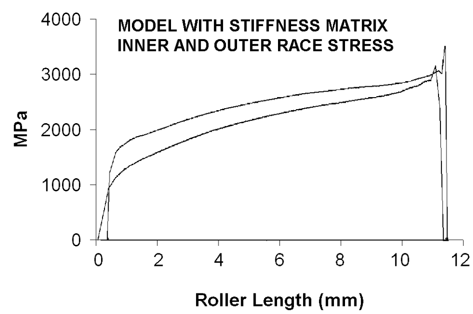

Figure 2 – Bearing Stress Comparison – Model vs. Model with Stiffness Matrix

Product Modeling - Bearing/System - Structural Analysis

Another example of FEA usage is in the structural evaluation of wheel bearing/ hubs. In addition to bearing performance, structural durability of integrated wheel hubs must be evaluated. A typical assembly is shown in Figure 3.

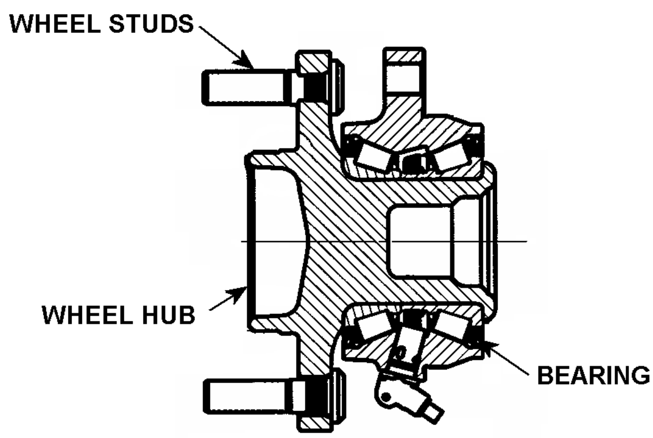

Figure 3 – Integrated Bearing/Wheel Hub Assembly

Using Abaqus/Standard, the wheel hub was modeled by a number of eight-node brick elements. Roller loads are calculated and applied to the bearing races. Contact interference of the bearing and the hub, along with the roller loads, produce stresses in the hub that can then be evaluated before prototyping begins. The analysis results are used to save cost and time in development of these wheel-end assemblies.

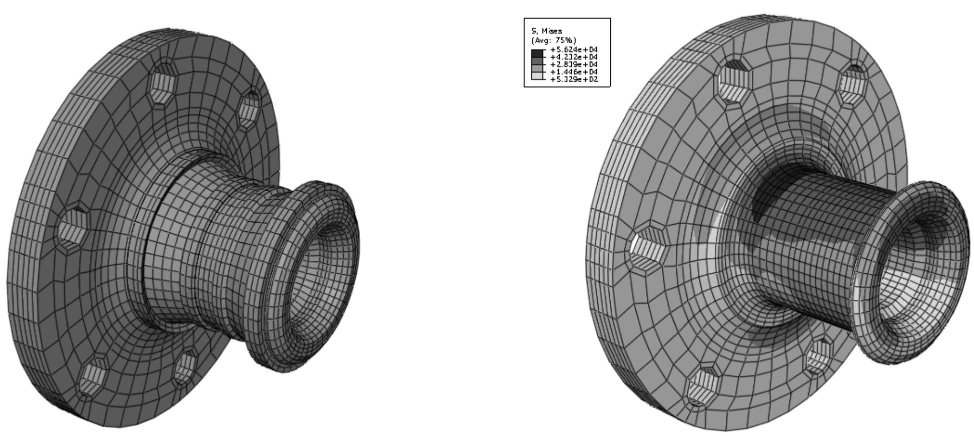

Figure 4 – Wheel Hub Assembly FEA Model and Hub Stress Results

Process Modeling - Ring Rolling

Metal shaping processes are modeled as well as product modeling. The analysis results offer better tooling design and reduce process trial costs. The process presented involves shaping the cross section of a ring between a mandrel and forming rolls and is illustrated in Figure 5 (ASM Metals handbook, 2005).

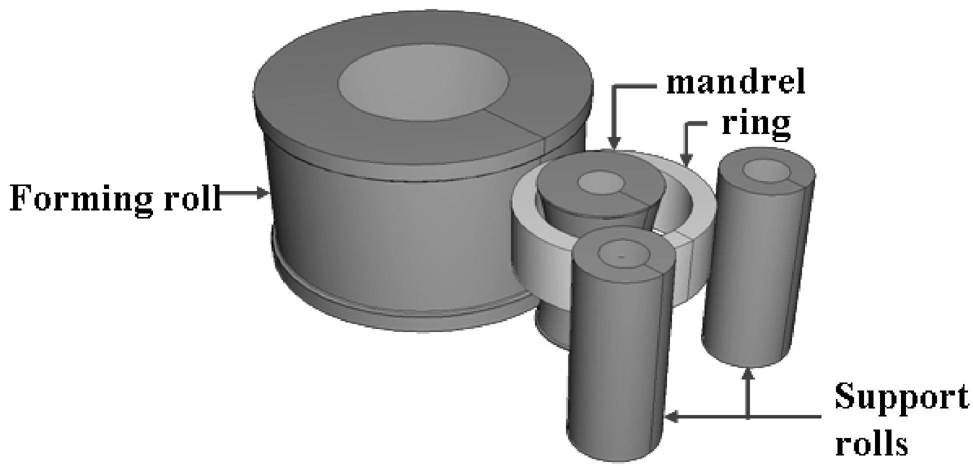

Figure 5 – Ring Rolling Process Sketch

Ring rolling is performed to create products ranging from CV cages to bearing double race cups. Figure 6 shows the process steps for production of a CV cage. The process starts with a ring that is cold rolled to achieve the specified cross-sectional profile. The pockets are then pierced out as a finishing operation.

Figure 6 – Ring Rolling Process Steps for Creating a CV Cage

Ring rolled double race cups are created in a similar manner. The process starts with a ring, which is then ring-rolled to a cross-sectional shape as shown in Figure 7.

Figure 7 – Ring Rolling Process Steps for Creating a Double Race Cup

For both ring-rolled parts, the model is setup as shown in the Figure 8. The king roll, which is modeled as an analytical rigid, is rotated at a certain speed while the mandrel is translated radially into the ring ID. The mandrel is also modeled by an analytical rigid. The ring is modeled by a number of elastic-plastic three dimensional eight-node elements. The ring is supported at the ID by a free spinning mandrel. The ring is also supported at the OD by two additional support rolls.

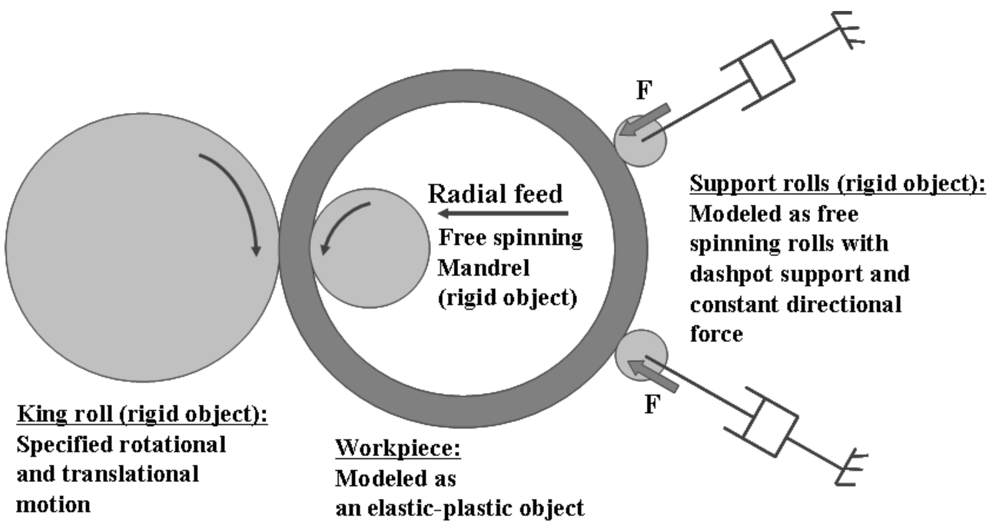

Figure 8 – Finite Element Model of Ring Rolling Process

The model was solved using the explicit solver. The explicit formulation is based on equations of dynamics (Sawamiphakdi, 2002)(Abaqus, 2007).

$$[M]\{\ddot{u}(t)\} = \{P_{ext}(t)\} - \{P_{int}(t)\} \tag{1}$$

[M] is the mass matrix, {Pext(t)} is the applied load vector, {Pint(t)} is the internal force vector and $\ddot{u}$ (t) is the acceleration vector at time t. The equations of motion are integrated using a central difference integration rule. The displacement vector at time t+Δt can be obtained from the previous displacement vectors and the acceleration vector at time t as follows:

$$\{u(t+\Delta t)\} = [\,2\{u(t)\} - \{u(t-\Delta t)\}] + (\Delta t)^2 \{\ddot{u}(t)\} \tag{2}$$

$$\{u(t+\Delta t) = [2\{u(t)\} - \{u(t-\Delta t)\}] + (\Delta t)^2 [M]^{1} [\{P_{ext}(t)\} - \{P_{int}(t)\} \tag{3}$$

Here {u(t+Δt)}, {u(t)}, {u(t-Δt)} are displacement vectors at time (t+Δt), (t) and (t-Δt) respectively and Δt is the time increment. The mass matrix [M] is a diagonal matrix and therefore its inversion is straightforward. Consequently, the above set of equations can be solved without iterations. However, the explicit procedure is conditionally stable. Stability in explicit procedure can be ensured by introducing a condition that the time increment is smaller than the time required for a dilational wave to cross any element in the mesh.

$$\Delta t \le \Delta t_{max} = \frac{L}{C_d} \tag{4}$$

$$C_d = \sqrt{\frac{E}{\rho}} \tag{5}$$

L is a characteristic element dimension, C_d is the dilational wave speed of the material, E is Young's modulus and ρ is the material density. Stable time increments in the explicit procedure are typically very small compared to the cycle time of forming processes. Therefore, an analysis of a typical metal forming process using the explicit procedure requires more than a million time increments. However, the computation time for each time increment in the explicit procedure is very short due to the diagonal mass matrix and the fact that the solution requires no iterations. Therefore, the run time is significantly reduced compared to the analysis using the implicit procedure. The run time of the explicit program can be further reduced using the following two techniques:

1. Artificially increasing forming rate: The speed of the forming roll and mandrel can be artificially increased to reduce the cycle time. This option is very effective for cold-forming processes. However, it may not be accurate for hot forming processes in which material flow stresses are strain-rate dependent.

2. Mass scaling: The mass of the workpiece can be increased by a scaling factor to reduce the wave front speed and to increase the stable time. Care must be taken to ensure that the increased mass does not cause unstable dynamic behavior due to inertia effects. This option can be used for modeling cold, warm and hot forming processes (Sawamiphakdi, 2002).

For the ring-rolling process of a CV joint, the steel ring of 53.67 mm OD, 41.885 mm ID and 37.948 mm wide is used as the starting ring. The forming roll rotated at 150 rpm, and the mandrel radial speed varied from 0.9 to 1.25 mm/sec. The duration of the forming cycles was six seconds. The initial step for ring rolling a CV joint is presented in Figure 9 and the final step is presented in Figure 10.

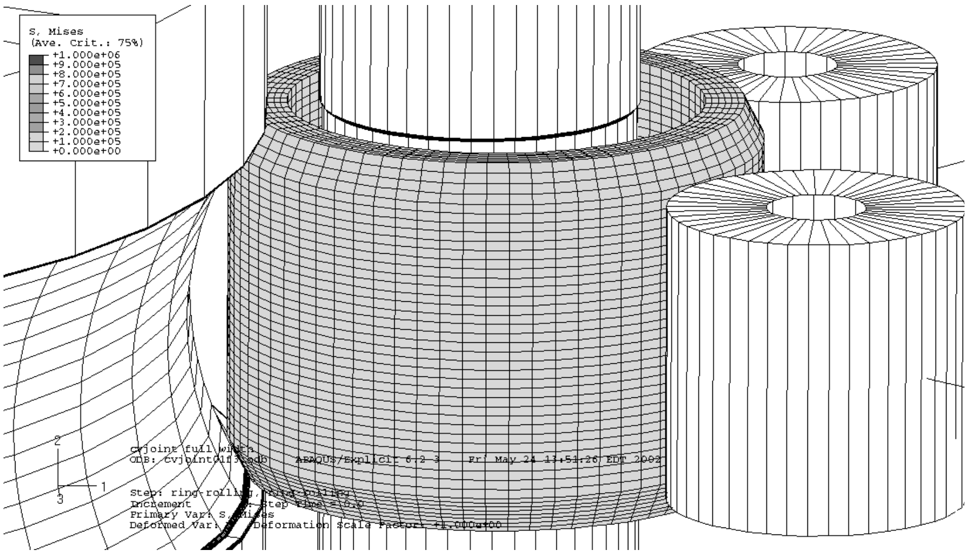

Figure 9 – Ring Rolling Model of CV Cage at Initial Step

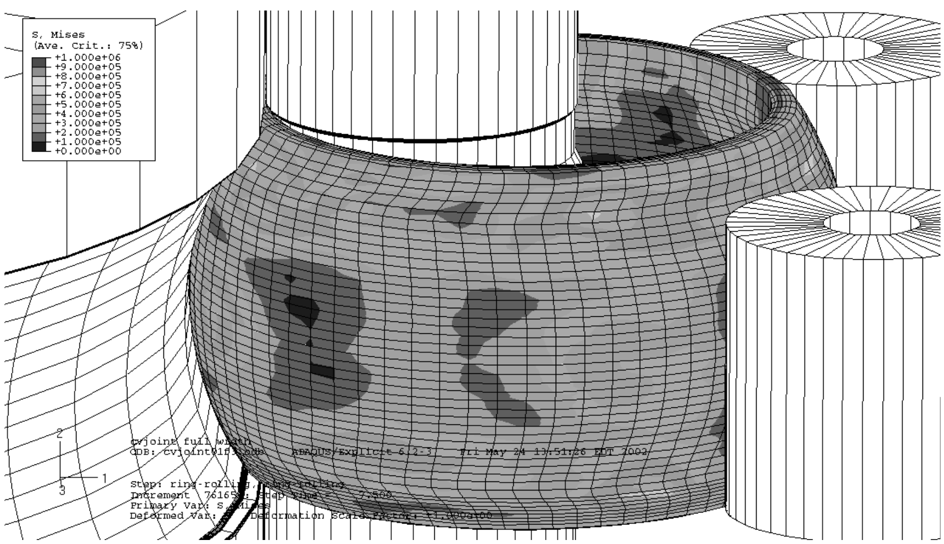

Figure 10 – Ring Rolling Model of CV Cage at Final Step

FEA results compared favorably to the experimental results. In Figure 11, FE predictions are compared with actual measurements. The actual measurements are shown in parenthesis.

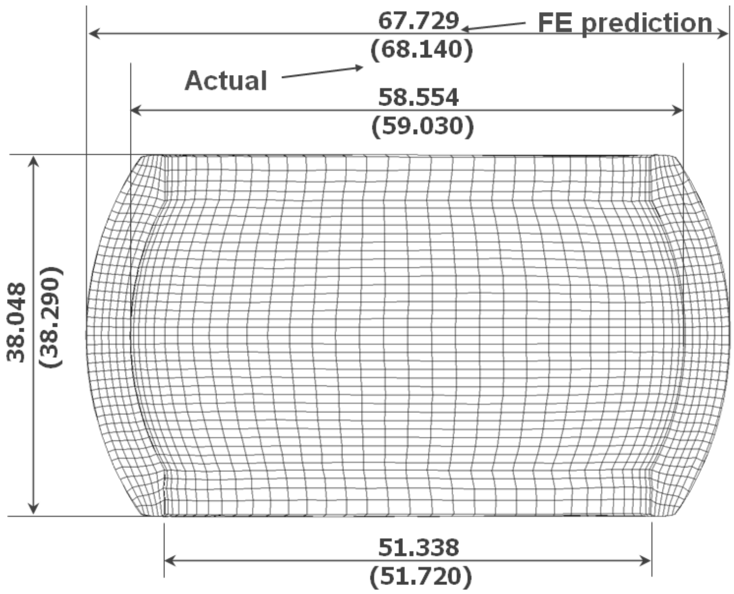

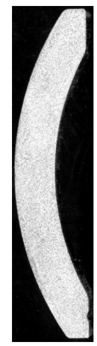

Actual Cross Section

Figure 11 – CV Cage FE vs. Actual Measurement Comparison

The ring rolling FE model for the double race cup was similar to the CV cage model. The analysis results are presented in Figure 12. The analysis results show that there was an underfilled region at the cup OD. The experimental results confirmed the underfilled phenomena. The predictions as well as the actual measurements are shown below with the actual measurements in parenthesis.

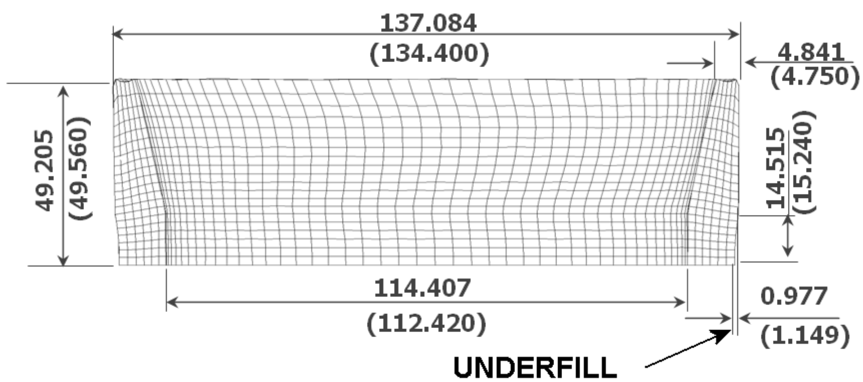

Actual Cross Section

Figure 12 – Double Race Cup FE vs. Actual Measurement Comparison

Revising the ID tooling removed the underfilled condition as shown in Figure 13. Since material between the two races at the ID is not needed to support the rollers, this material can be pushed outward to fill the underfill of the OD. Actual measurements are shown in parenthesis. For all these examples, the accuracy of the profile is within one mm.

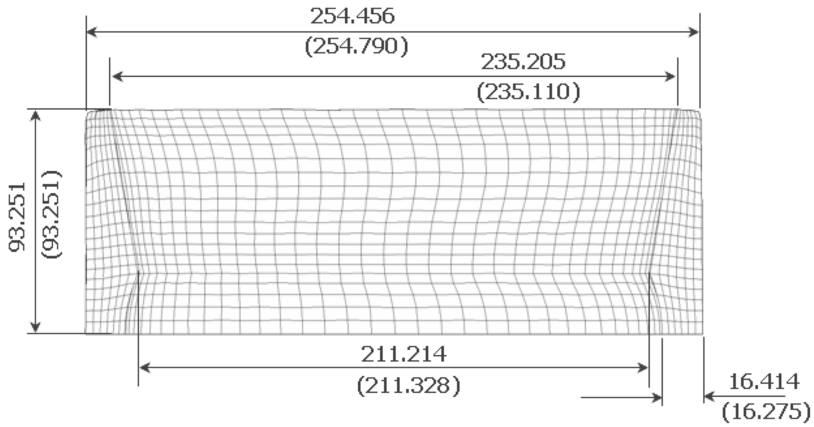

Figure #13 – Revised Double Race Cup FE vs. Actual Measurement Comparison

Process Modeling - Tube Elongating Process

The second process to model is the tube elongating process. The Assel elongating mill is employed to reduce thick-walled tubes to near finished dimensions. The system consists of three forming rolls spaced 120 degree apart around the main axis and a mandrel as shown in Figure 14. Each roll is inclined to the main axis about 3-5 degrees, and the feed angle of each roll varies from 9-12 degrees. The tube is drawn into the mill in a spiral motion by the action of the rolls. The tube diameter is reduced in the inlet zone ahead of the roll shoulder where the tube is gripped, rotated and drawn into the mill (McGannon, 1971).

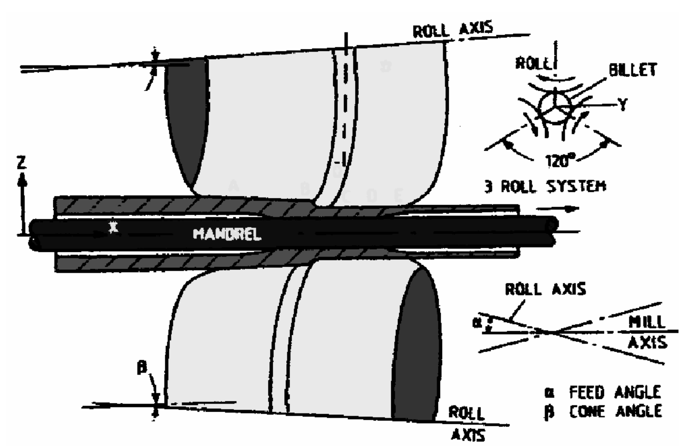

Figure 14 – Typical System of Assel Elongating Mill

The finite element analysis was carried out using Abaqus/Explicit. A three-dimensional finite element model representing the Assel elongating process was developed using Abaqus/CAE. The model consisted of three rolls, a tube, a mandrel and a support. The rolls, mandrel and support were modeled as analytical rigid surfaces. The tube was modeled using elastic-plastic three dimensional elements. The initial results are presented in Figure 15 and the final results are presented in Figure 16.

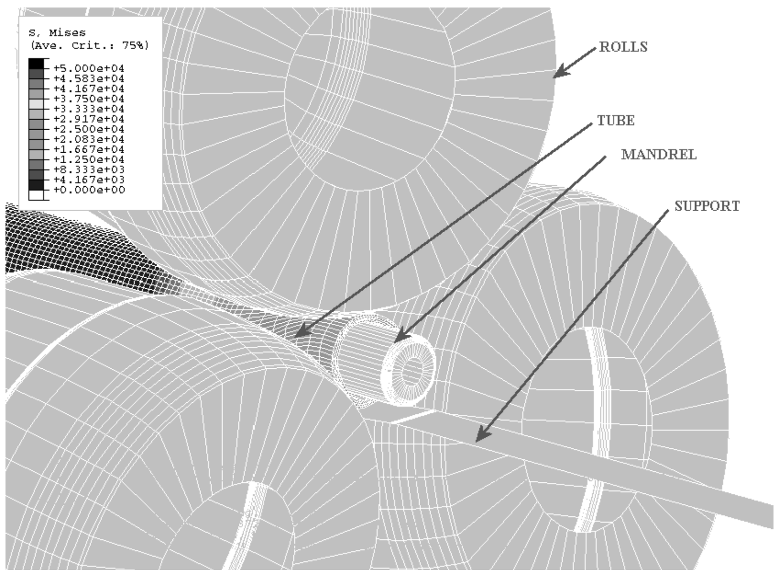

Figure 15 – Finite Element Model of Tube Elongating Process

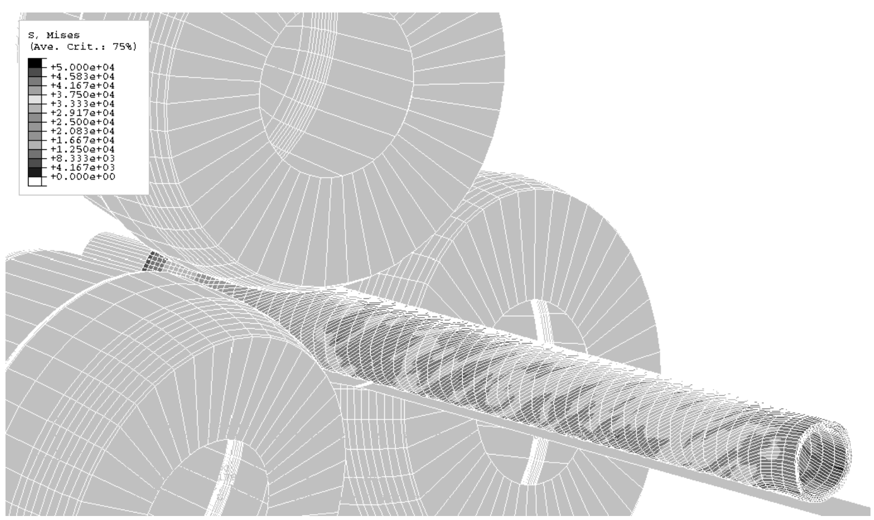

Figure 16 – Finite Element Analysis Results of Tube Elongating Process

Process Modeling - Tube Straightening

Another process that benefits from this type of analysis is tube straightening. In this process, the tube is fed between five rolls as shown in Figure 17. The bottom two rolls are mechanically rotated at a certain speed while the top three rolls are free to rotate. Top and bottom rolls are tilted in opposite directions in order to pull the tube through the system. The tube is plastically deformed in opposite directions due to the spinning between the rollers and results in a straightened tube (McGannon, 1971).

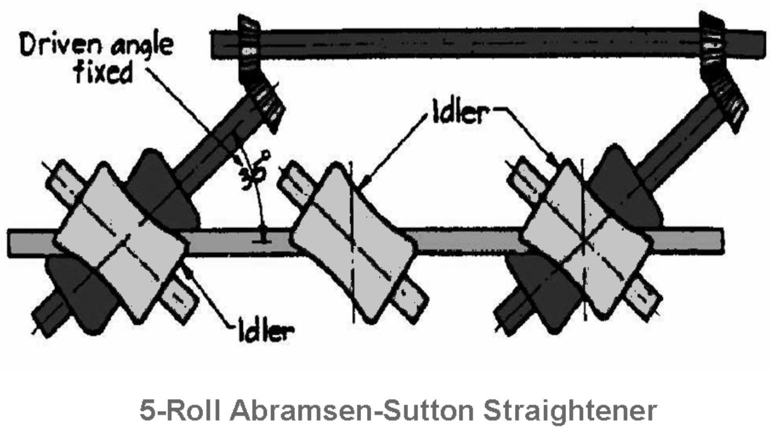

Figure 17 – Finite Element Modeling of Tube Elongating Process

The finite element model is presented in Figure 18. The steel tube is modeled by a number of three dimensional hexahedron elements. The rollers are modeled as rigid analytical surfaces. The calculated roll forces are plotted in Figure 19.

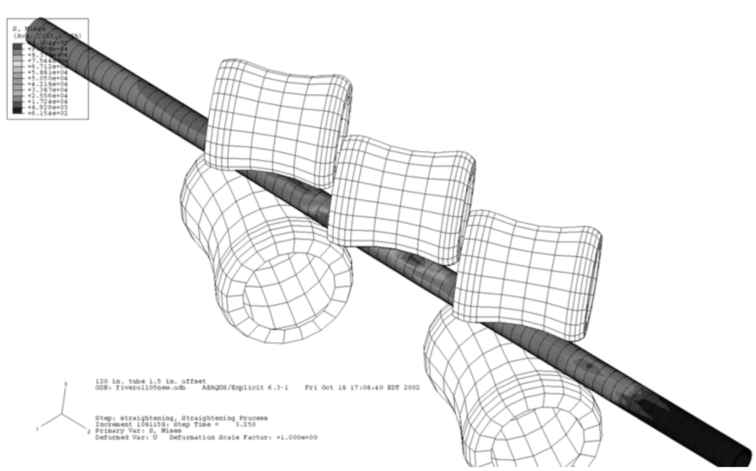

Figure 18 – Tube Straightening Process – FiniteElement Model

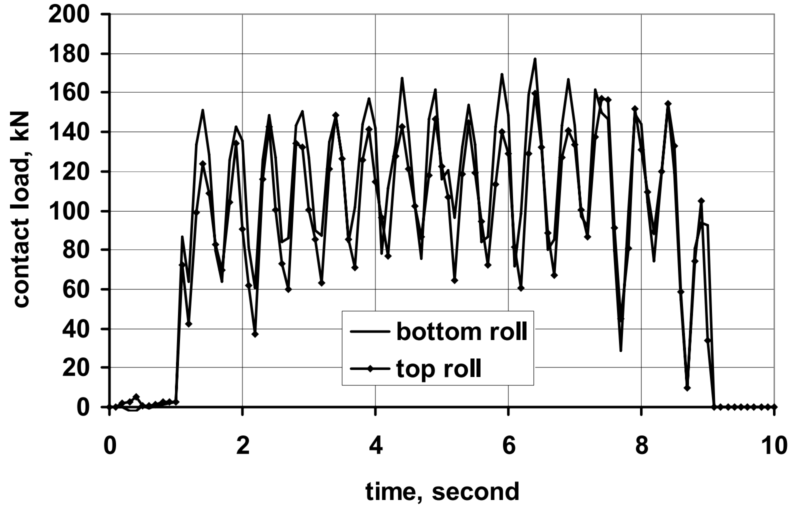

Figure 19 – Calculated Roller Force Graph

Material Modeling - Non-metallic Inclusions in Steel

An important aspect of bearing performance is material cleanness. Non-metallic inclusions (NMI) in the bearing steel can have a detrimental affect on bearing life. To better understand the effect of NMI on bearing life, finite element models have been created to determine stresses around them as shown in Figure 20. Since the inclusions are small relative to the bearing race, a small control volume is created around the inclusion. The applied hertzian pressure and boundary stresses are applied around the volume using a user subroutine in Abaqus/Standard (Johnson, 1985).

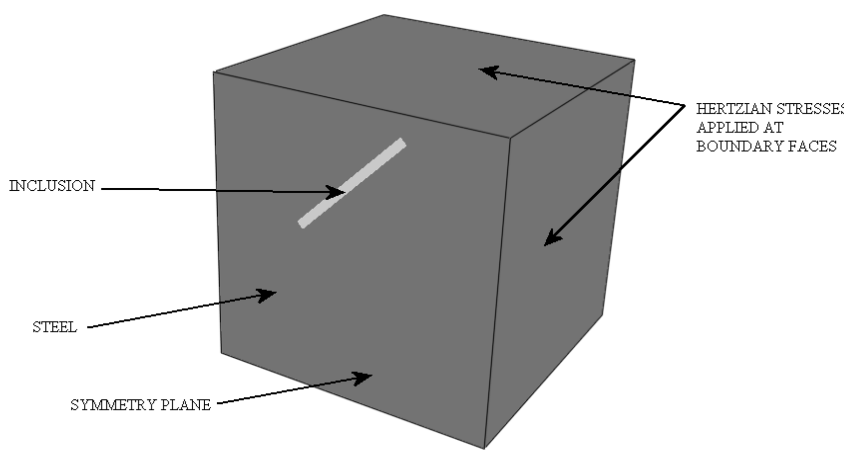

Figure 20 – Inclusion/Steel FEA Model

The inclusion material properties are defined and a fine mesh is used. Weak springs are used to constrain any rigid body motion due to round off errors creating force imbalance. The model is solved to determine the distribution of stresses due to hertzian contact pressure. Several models are created for different inclusion sizes, orientations relative to the surface and depth location. These models show how inclusion geometry affects the stress field. The Von Mises stress contour plot of the volume is shown in Figure 21. The inclusion with its higher stiffness properties creates a stress riser at the maximum hertzian stress pattern. By comparing the stresses of this model with stresses of a model without inclusions, a relative life factor can be determined.

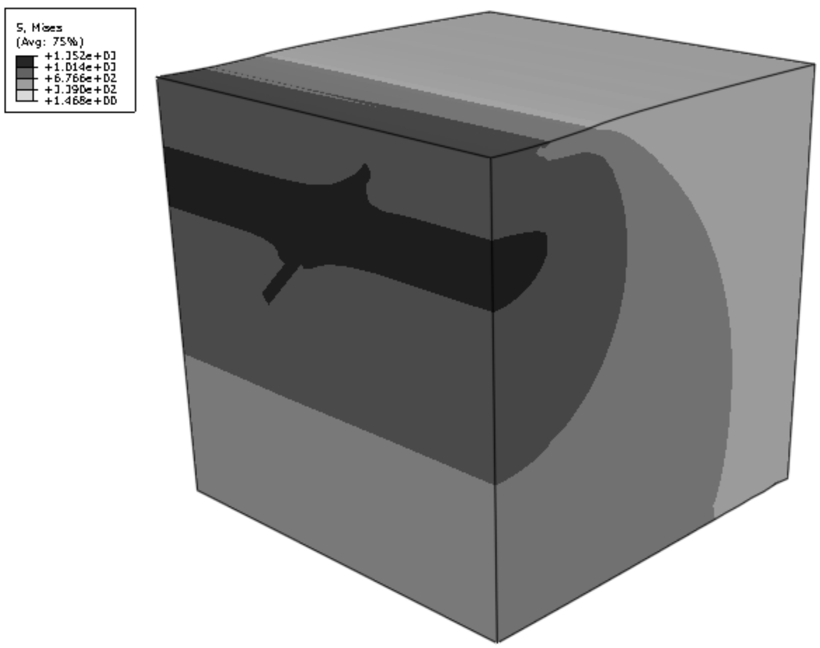

Figure 21 – Inclusion/Steel FEA Model Stress Contour Plot

CONCLUSION

Finite element modeling has been utilized to efficiently develop products and processes at The Timken Company. In product analysis, FEA results are used to evaluate structural designs of bearing integrated components. Models range from macroscale analysis of wheel hubs to microscale analysis of inclusions in steel. A user subroutine to apply Hertzian contact pressure and boundary stresses was employed successfully to reduce the size of models and offer accurate results. Process analysis results indicate that three-dimensional incremental forming processes can be analyzed successfully using the explicit solver with excellent accuracy and in a relatively short run time. Mass scaling can be employed to increase the stable time increment in the explicit program and to reduce the computational time.

Acknowledgements:

The authors would like to thank the many researchers whose work is compiled in this paper. These include P.M. Pauskar, D.Q. Jin, Tony Perez, Justin Bill from The Timken Company, Tim Mason from Dassault Systems, Erie and Erick Alley from Georgia Institute of Technology.

References:

1. Timken, Automotive Bearing Applications Manual, 1985.
2. Timken, SYBER Reference Manual, 2007.
3. ABAQUS Inc., *ABAQUS User's Manual Version 6.7.1*, 2007.
4. K. Sawamiphakdi, P.M. Pauskar, D.Q. Jin and G.D. Lahoti, "Ring rolling process modeling using explicit finite element analysis." Proc. 7th International Conference on Technology of Plasticity, Yokohama, Japan, pp. 859-864, Oct. 27-Nov 1, 2002.
5. Metals Handbook, Volume 14A, 10th ed., 2005.
6. The Making, Shaping and Treating of Steel, Ed by Harold E. McGannon, Ninth Edition, 1971.
7. K. Sawamiphakdi, D.Q. Jin and A. J. Lahoti, "Overview of 3D Finite Element Modeling in Tube Making Process at The Timken Company".
8. Johnson, K.L., Contact Mechanics, Cambridge Univ. Press, pp. 99-104, 1985.